Geomechanics and Engineering, *Vol. 9, No. 6 (2015) 815-827*
DOI: http://dx.doi.org/10.12989/gae.2015.9.6.815

DEM analyses of the mechanical behavior of soil and soil-rock mixture via the 3D direct shear test

Wen-Jie Xu*, Cheng-Qing Li and Hai-Yang Zhang

State Key Laboratory of Hydroscience and Hydraulic Engineering, Department of Hydraulic Engineering, Tsinghua University, Beijing, China 100084

(*Received December 17, 2014, Revised October 28, 2015, Accepted October 31, 2015*)

Abstract. The mechanical behavior of soil and soil-rock mixture is investigated via the discrete element method. A non-overlapping combination method of spheres is used to model convex polyhedron rock blocks of soil-rock mixture in the DEM simulations. The meso-mechanical parameters of soil and soil-rock interface in DEM simulations are obtained from the in-situ tests. Based on the Voronoi cell, a method representing volumtric strain of the sample at the particle scale is proposed. The numerical results indicate that the particle rotation, occlusion, dilatation and self-organizing force chains are a remarkable phenomena of the localization band for the soil and soil-rock mixture samples. The localization band in a soil-rock mixture is wider than that in the soil sample. The current research shows that the 3D discrete element method can effectively simulate the mechanical behavior of soil and soil-rock mixture.

Keywords: soil-rock mixture (S-RM); discrete-element modelling (DEM); failure; shear strength; deformation; localization

1. Introduction

Soil-rock mixture (S-RM) is one type of complex geotechnical material, which distributes widely in natural. For the large rock blocks, the mechanical behavior of S-RM is more complicated than that of soil.

Although there are many criticisms of the direct shear test (Terzaghi and Peck 1848, Morgenstern and Tchalenko 1967), in terms of simplicity and lower cost, the test is still one of the commonly used testing method for determining the strength parameters of geotechnical materials (Oyanguren *et al*. 2008, Ishida *et al*. 2010). To study the mechanical properties of the S-RM of a slope in Yunnan province, China, a series of large scale direct shear tests (60 cm × 60 cm × 80 cm) were conducted by Xu *et al*. (2011). Although, these field tests have provided a thorough understanding of the properties of S-RM, it is very difficult or even impossible to perform a systematic study of the mechanical behavior and failure processes of S-RM via the traditional testing methods.

Alternatively, numerical methods, such as finite element method (FEM) and discrete element method (DEM) have great advantages for understanding the mechanical behavior of geotechnical

*Corresponding author, Associate Professor, E-mail: wenjiexu@tsinghua.edu.cn

http://www.techno-press.org/?journal=gae&subpage=7 ISSN: 2005-307X (Print), 2092-6219 (Online)

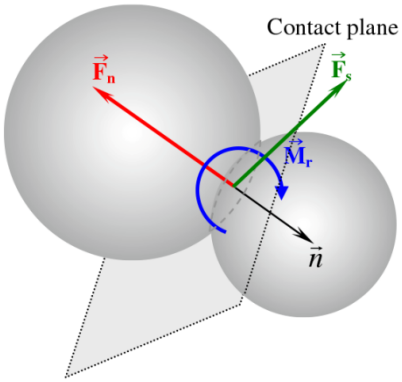

Fig. 1 Two spheres in contact: $\vec{F}_s$ is tangential contact force vector, $\vec{F}_n$ is normal contact force vector, $\vec{M}_r$ is contact moment vector, $\vec{N}$ is contact normal vector (Widuliński *et al*. 2009)

materials in the meso-mechanical scale. In particular, the DEM provides strong insights into the strength and deformation properties of granular materials (Cundall and Strack 1979, Potyondy and Cundall 2004, Sullivan 2008, Evans and Frost 2010, Scholtes and Donzé 2012).

In this study, the generation method of the DEM numerical model of S-RM is proposed based on the in-situ tests of Xu *et al*. (2011). Then, a series of 3D DEM numerical tests of soil and S-RM samples are conducted, and the difference of the meso-mechanical behavior between soil and S-RM are studied.

2. DEM and YADE

In the DEM, a solid material is represented as an assembly of particles which interact with each other. The macro mechanical behavior of soil is reproduced by determining the meso properties of the particles, such as the interaction forces. In this study, YADE is used as the DEM simulation program, which is an open source DEM code based on three dimensional DEM (Kozicki and Donzé 2008, 2009). In YADE, the soft-particle approach is used, in which the particle deformation is represented by inter-particle overlap.

In addition, the cohesive particle model is used in the current DEM model, which can be used to simulate the cohesive-frictional material like geotechnical materials. Furthermore, to simulate the rotation of spheres, the inter-particle moments (Fig. 1) have been included in the cohesive particle model of YADE, in which the rolling moments between particles are transferred through contacts resisting particle rotations (Kozicki and Donzé 2008, 2009, Widuliński *et al*. 2009).

3. Generation of 3D DEM model

3.1 Effect reinforcement

The structural characteristics of S-RM, such as shape of the rock block, particle distribution and rock block content, can greatly influence its mechanical behavior. Generating a meso-structural model is an important step for for numerical analyses of the meso-mechanics of S-RM. A 3D

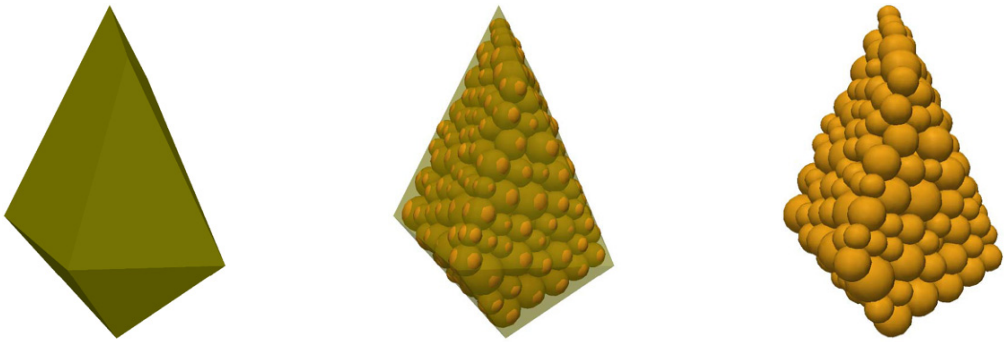

(a) (b) (c)

Fig. 2 Schematic view of the convex polyhedron rock block using the non-overlapping combination of spheres: (a) geometry of rock block; (b) rock block filled with spheres; (c) rock block represented by spheres

random meso-structure modelling system of S-RM (R-SRM^{3D}) was developed by Xu (2008), which can generate S-RM models with arbitrary convex polyhedron rock blocks, according to their rock block size distribution, content and other parameters.

Spherical particles are widely used in 3D DEM models, and there are two methods to represent irregular particles based on the sphere assembly. One is the non-overlapping combination, in which no overlap is permitted between spheres (Mcdowell and Harireche 2002, Matsushima *et al*. 2009, Jerier *et al*. 2010, Ergenzinger *et al*. 2012); the other method is the overlapping combination, in which two adjacent spheres can overlap with each other (Chang *et al*. 2003, Garcia *et al*. 2009). Furthermore, in recent years a spheropolyhedra approach has been development to simulate the polyhedron blocks in DEM (Galindo-Torres and Pedroso 2010). In this study, the former method is used to describe the convex polyhedron rock blocks (Fig. 2), which can be used to simulate the breakage of rock blocks. The generation process is implemented in YADE as follows.

Firstly, a dense packing of spheres with radius ranging from R_{min} to R_{max} in a given geometric model of the rock block is generated randomly using YADE. The geometric surfaces of the rock block are used as the fixed boundaries. Then, sufficient numbers of DEM interaction steps are performed, until the whole granular system reaches an equilibrium state. In this process, the solid spheres can fill in the rock block. During the numerical simulation, the inter-particle friction angle is set to zero, and the elastic modulus and Poisson ratio of particle contact are set the same as that of the rock material in the following DEM simulations.

In this study, an S-RM sample (Xu *et al*. 2011) with rock block content of 30% is selected (Fig. 3). According to the size and rock block distribution in the in-situ tests, a S-RM sample includes 464 rock blocks is generated by the R-SRM^{3D} (Fig. 4(a)). Fig. 4(b) shows the corresponding assemblies of spheres with diameter in the range of 1.2 ~ 1.9cm. Soil among the rock blocks is represented by spherical particles with diameter in the range of 0.6~1.8 cm, and the void ratio of the "soil" is 0.4. Fig. 5(a) shows the cross-section of the S-RM model with 148, 589 spheres.

Furthermore, an soil model is designed to reproduce the same physical and mechanical properties of the "soil" in S-RM as that of the in-situ test. Thus, the distribution of sphere radius representing the soil sample is set the same as that of the S-RM sample, and 168,676 spheres were generated (Fig. 5(b)).

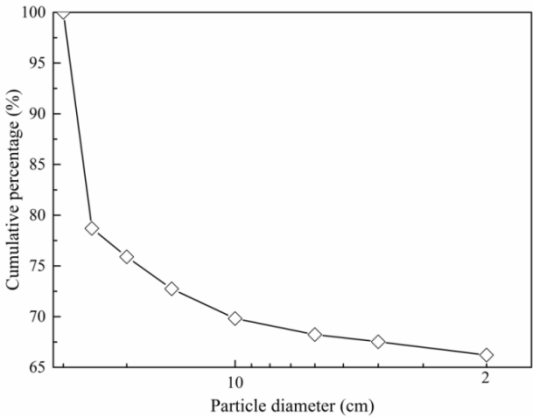

Fig. 3 Size distribution curve of the rock block in the S-RM sample

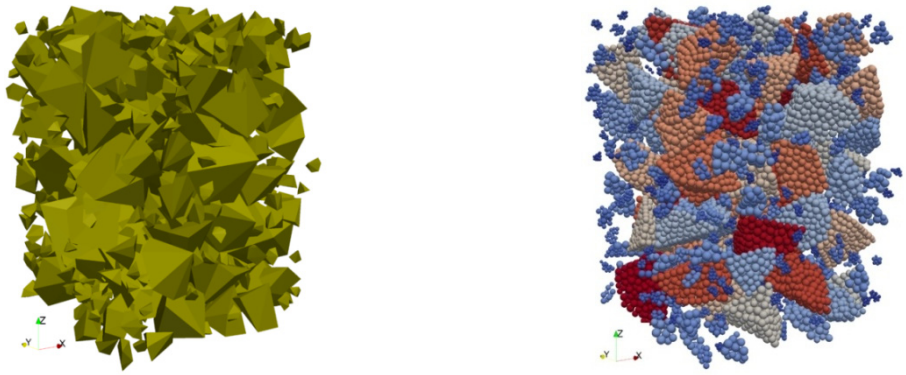

(a) (b)

Fig. 4 3D spatial structural model of rock blocks in the S-RM model: (a) convex polyhedron S-RM rock blocks generated by R-SRM^{3D} program; (b) convex polyhedron S-RM rock blocks model described with clumps of spheres

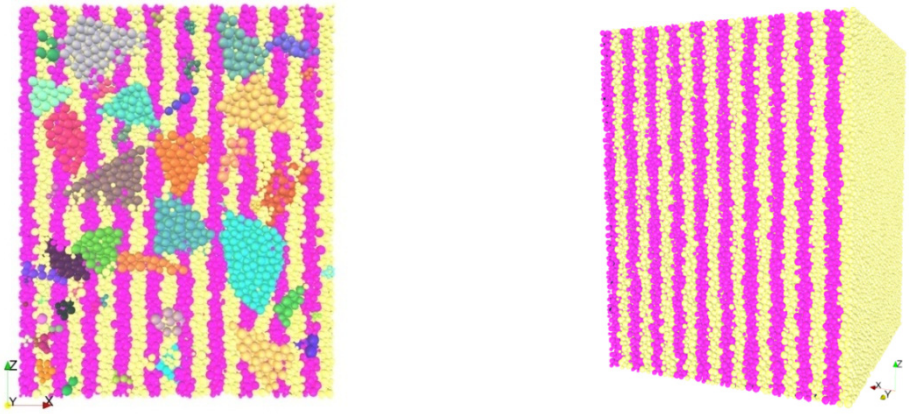

(a) (b)

Fig. 5 Numerical model of soil and S-RM samples: (a) middle cross-section of S-RM sample; (b) soil sample

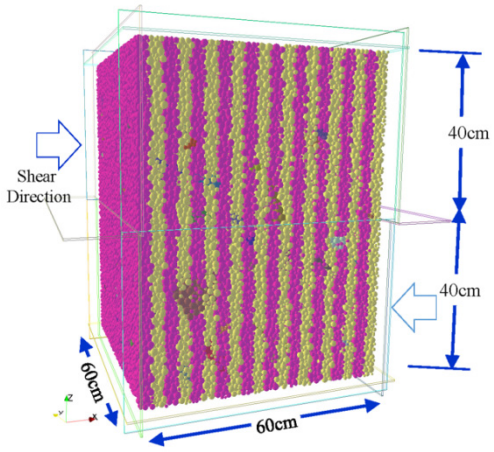

Fig. 6 DEM model of a direct shear box

4. DEM simulation of direct shear test

The upper and lower shear boxes of the direct shear test model consist of five walls, as shown in Fig. 6. To avoid particles escaping from the shear box, two walls are used to close the horizontal surfaces on both sides of the shear plane. During the shearing process, these two walls move together with the upper and lower shear boxes, respectively.

Firstly, the sample is consolidated under a specified normal stress, which is applied by moving the top wall slightly downwards, until the reaction force in the z direction on the upper wall reaches the aimed values. During the shearing process, the upper and lower shear boxes are moved in the positive and negative directions of the x axis, respectively, at a constant strain rate 10^{-5}/s. When the horizontal strain reaches 25% (equal to that of the in-situ test), the shear test is finished. During the whole process, the normal stress is maintained at the target values (tolerance of 10^{-5}) through a servo-control mechanism of the top wall.

A workstation with 12-core processors (CPUs) and 64G memory is used in this study. And the calculation time of each DEM numerical test is about 16 hours.

5. Meso-mechanical parameters

5.1 Meso-mechanical parameters of the soil particles

In Xu *et al*. (2011), three tests with different normal stresses (13.9, 25.2 and 32 kPa) were carried out for soil samples. To obtain the meso-mechanical parameters of the soil particles in DEM numerical tests, two DEM direct shear tests with different normal stress (13.9 and 32 kPa) are performed. By adjusting the meso-mechanical parameters of the soil particles, the development of the shear stress with the shear strain is obtained from DEM numerical tests, which can match that of the in-situ tests well. As the surfaces of shear box used in Xu *et al*. (2011) are rough, in all the DEM tests, the friction angle of the shear boxes is set as 8.0°. The shear boxes are taken to be rigid walls, and the elastical modulus is set to ten times that of the rock blocks. Table 1 shows the obtained meso-mechanical parameters of the soil particles and the shear box.

Table 1 Parameters of soil particles and shear box used in DEM simulations

Material	Parameter	Value
Soil	Density of particle, ρ (kg/m^3)	2,350
	Elastic modulus of particle contact, E_c (MPa)	40
	Poissons's ratio of particle contact, v	0.05
	Friction angle of particle, μ (°)	18.0
	Cohension, c (kPa)	5.0
Shear box	Elastic modulus of contact, E_c (GPa)	6
	Poissons's ratio of contact, v	0.1
	Friction angle, μ(°)	8.0

Notes: the normal stiffness K_n and tangential stiffness K_s, can be calculated from $K_n = E_c \dfrac{2R_A R_B}{R_A + R_B}$ and $K_s = E_c v_c \dfrac{2R_A R_B}{R_A + R_B}$, respectively, with R_A and R_B being the radii of the two spheres in contact.

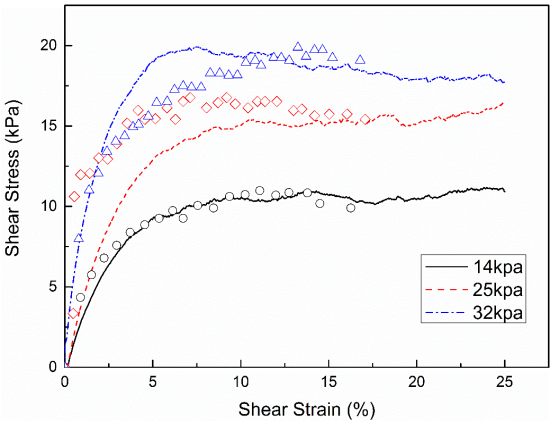

Fig. 7 Relationship of shear stress - shear strain for soil (hollowed points represent results from in-situ direct shear tests)

Fig. 7 shows the relationship between shear stress and shear strain for the soil samples under three different normal stresses. From Fig. 7, it can be observed that except for the test with normal stress of 25 kPa the difference is larger at the beginning of the curve, other curves obtained from DEM tests match well the results of in-situ tests. There may be some measurement errors for the in-situ test with the normal stress of 25 kPa, because at the beginning of the test, the shear stresses are larger than 32 kPa, which is improper.

5.2 Meso-mechanical parameters of the rock particles and soil-rock interface

According to the in-situ tests in Xu *et al*. (2011), there is no breakage for higher-strength rock blocks. Furthermore, according to the field observation there is no cohesion between soil and rock particles. Thus, in the current DEM numerical test, every rock block is regarded as a rigid clump

Table 2 Parameters of rock particles and soil-rock interface used in DEM simulations

Material	Parameter	Value
Rock	Density of particle, ρ (kg/m^3)	2,650
	Elastic modulus of particle contact, E_c (MPa)	600
	Poissons's ratio of particle contact, v	0.1
Soil-rock interface	Friction angle of particle, μ(°)	5.0
	Cohension, c(kPa)	0.0

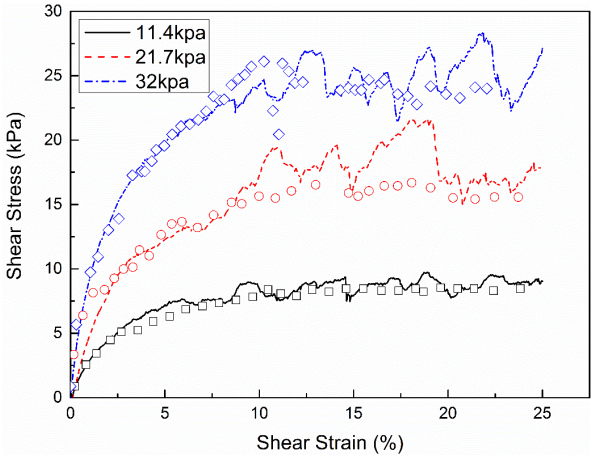

Fig. 8 Relationship of shear stress - shear strain for S-RM samples (hollowed points represent results of in-situ direct shear tests)

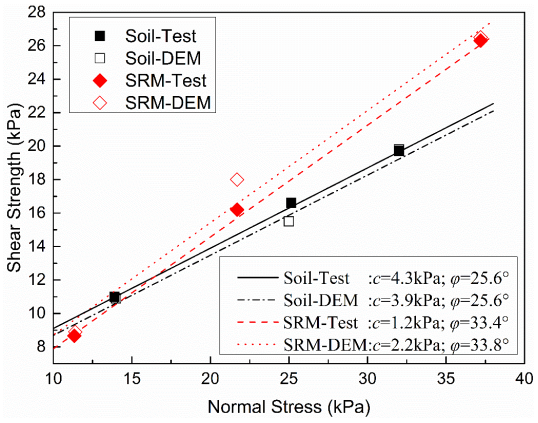

Fig. 9 Shear strength of soil and S-RM samples obtained form DEM simulations and in-situ direct shear tests

of spheres, and the cohesion of the soil-rock interface is set as zero. To determine the friction angle of the soil-rock interface, a DEM direct shear test of the S-RM sample with the normal stresses of 37.2 kPa is carried out. The friction angle of the soil-rock interface is adjusted until the shear stress

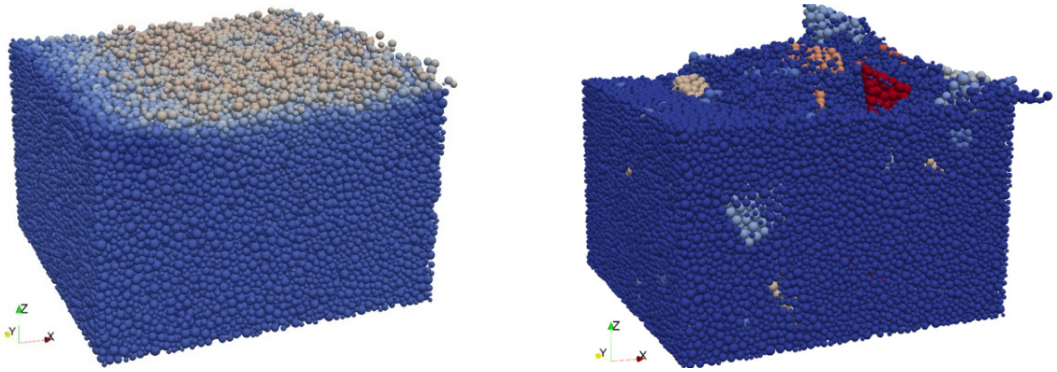

(a) (b)

Fig. 10 3D shear face of soil and S-RM samples: (a) Soil sample; (b) S-RM sample

~shear strain curve can match the in-situ tests. Table 2 shows the obtained meso-mechanical parameters.

Fig. 8 shows the shear stress~shear strain curves for S-RM samples under three different normal stresses obtained from the DEM and in-situ tests. It can be observed that the shear stress~shear strain curves of the S-RM sample obtained from DEM tests match well the results of in-situ tests.

Fig. 9 shows the relationship between the shear strength and normal stress of the soil and S-RM sample. For the soil and S-RM samples, the shear strength obtained from DEM numerical tests are similar to those that of in-situ test. Fig. 10 illustrates the shear face of the soil and S-RM samples obtained from DEM tests, which indicates that for the influence of the rock blocks the shear face of S-RM sample is undulating, while the soil sample is smooth. This increases the shear strength of the S-RM sample, especially as its friction angle is larger than that of the soil sample,

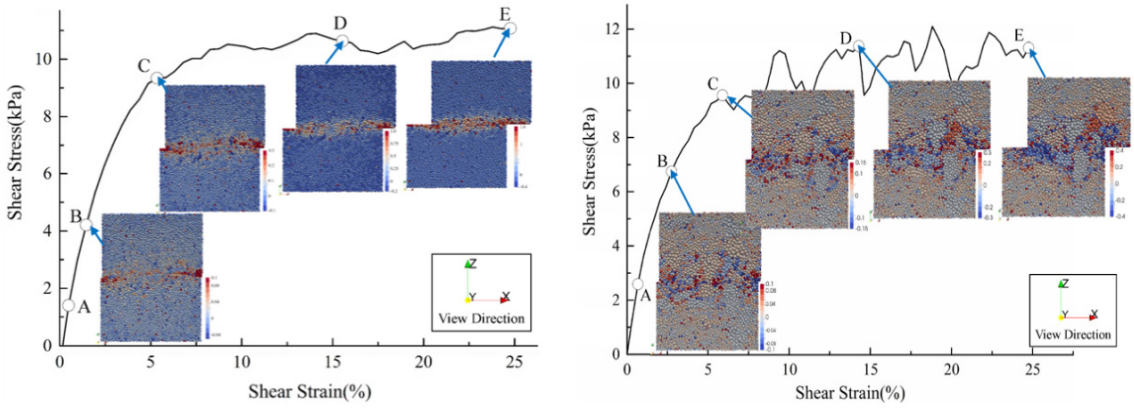

(a) (b)

Fig. 11 Evolution of particle rotation in middle cross-section of the sample along the *y* direction during shearing process: (a) Soil Sample, normal stress is 14 kPa; (b) SRM sample, normal stress is 11 kPa

6. Results and interpretation

One of the powerful advantage of the numerical test is that an reasonable numerical test can easily reveal the mechanical behavior and failure processes of geotechnical materials, which is very important to study their meso and macro mechanics. In this part, the particle rotation, development of the volume strain at meso-scale and Shear-induced anisotropy of the soil and S-RM sample are studied according the DEM numerical tests.

6.1 Particle rotation characteristics

Fig. 11 shows the evolution of particle rotation for the soil and S-RM samples. For both samples, particles around the shear plane show larger rotations other particles. For the soil sample, the rotation direction is mainly in the *y* direction. While for the S-RM sample, the rotation direction of the rock blocks is mainly in the y direction, however the rotation direction of the soil particles influenced by the neighboring rock blocks. Furthermore, the width of the "rotation localized zone" of S-RM sample is larger than that of the soil sample.

6.2 Development of the volume strain at meso-scale

To study strain of the spherical particle system, it is simplified and a Voronoi cell is used for each sphere particle. As we know, the particles can rearrange in the shearing process, which changes the structure and volume of the pores around the spherical particles. As a result, volume of the corresponding Voronoi cell of the sphere particle will change too. So, the variation in the volume of the Voronoi cell of each sphere can be used to describe the variation of the pore volume (or volume strain) near the spherical particles.

Firstly, according to spatial structure of the aggregation of spheres composing the sample at a specified time, Voronoi cell of each sphere particles can be generated (Fig. 12) using Voro++ (Rycroft 2009), an open source software library for the computation of the 3D Voronoi tessellation. Then, according to the volume of each Voronoi cell at a specified time, volumetric strain of each cell is calculated by Eq. (1) as

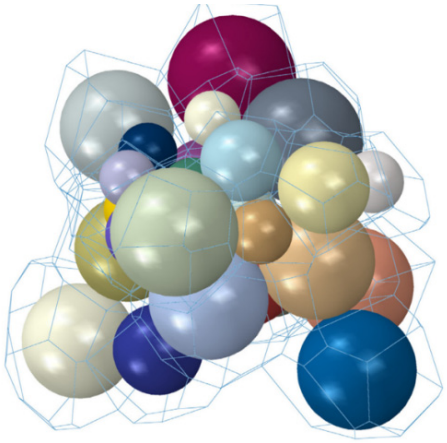

Fig. 12 Aggregation of spherical particles and corresponding Voronoi cells

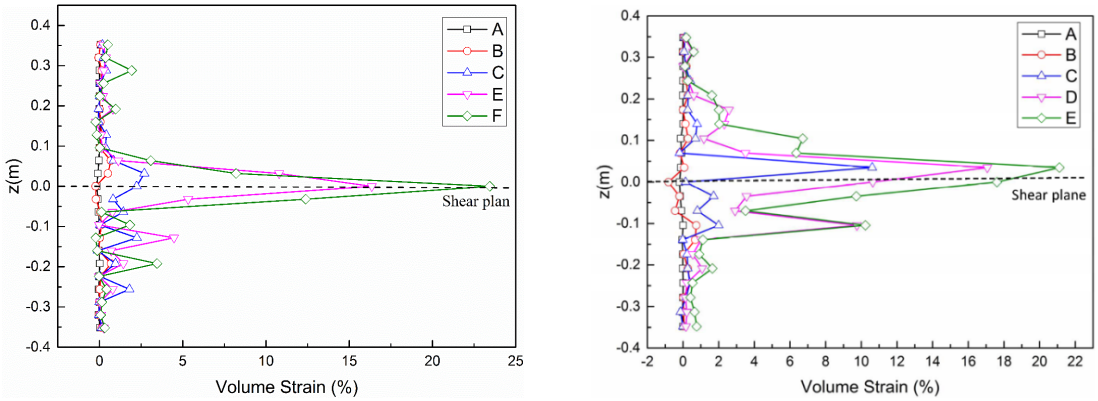

(a) (b)

Fig. 13 Evolution of volumetric strain of Voronoi cell (the curves A~E correspond to that of the Fig.11): (a) Soil Sample, Normal stress is 14 kPa; (b) S-RM sample, Normal stress is 11 kPa

$$\varepsilon_i^{voro}(t) = \frac{V_i^{voro}(t) - V_i^{voro}(0)}{V_i^{voro}(0)} \cdot 100\% \tag{1}$$

where, i is the sphere ID number composing the sample; $\varepsilon_i^{voro}(t)$ and $V_i^{voro}(t)$ are the volumetric strain and volume of the Voronoi cell corresponding the i^{th} sphere at time t, respectively; and $V_i^{voro}(0)$ is the volume of the Voronoi cell corresponding the i^{th} sphere at the beginning of the shearing process.

Fig. 13 shows that the development of the average volumetric strain ($\bar{\varepsilon}^{(z)_{voro}}$) of all the particles at different height, as calculated by Eq. (2)

$$\bar{\varepsilon}^{(z)}{}_{voro} = \sum \varepsilon_i^{voro} \Big/ N^{(z)} \tag{2}$$

where, ε_i^{voro}, $N^{(z)}$ are the volumetric strain of the i^{th} Voronoi cell and the total number of spherical particles with the coordinate z being in the range of $[z_i, z_{i+1}]$ at a specified time, respectively.

For both the soil and S-RM samples, the volumetric strain of the Voronoi cells of the particles around the shear plane increases sharply, forming a dilation zone. For the S-RM sample, the width of the dilation zone is around 40 cm, which is larger than that of the soil sample (around 20 cm). Outside the dilation zone, the volumetric strain changes very little or remains constant. According to the analysis results of Fig. 13, there is a "concentrated localization band" around the shearing surface. Outside of this "band", the volumetric strain changes sharply to very little and remains constant. Fig. 14 shows the deformation of the samples and the corresponding localization zone at the end of the simulations. It can be observed that the differential deformation is greatly larger in the dilation zone than other places for both samples. Furthermore, the width of the "dilation zone" is similar to that of the "rotation localized zone" in Fig. 11, and forms the "localization band".

6.3 Shear-induced anisotropy

Evolution of the anisotropies of normal contact force inside the localization band during the shearing process are illustrated in Fig. 15. It can be observed that the distribution of normal contact

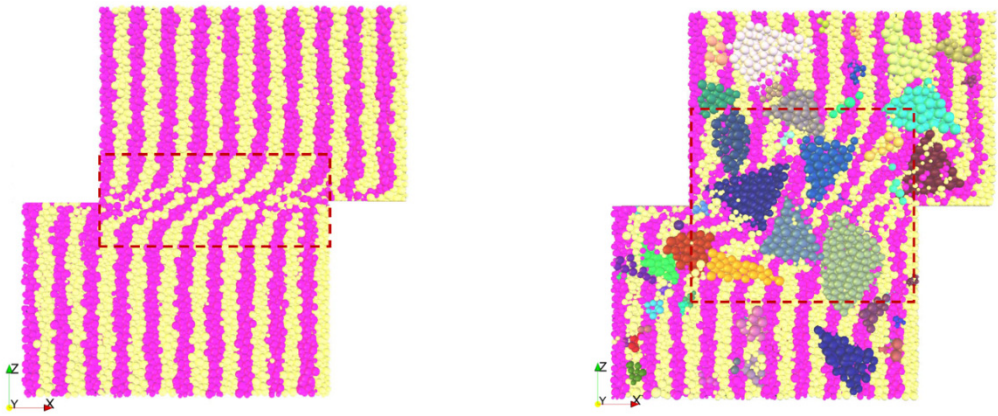

(a) (b)

Fig. 14 Sample deformations in middle cross-section (dashed line box is the dilation zone according to Fig. 12): (a) soil sample, Normal stress is 14 kPa; (b) S-RM sample, Normal stress is 11 kPa

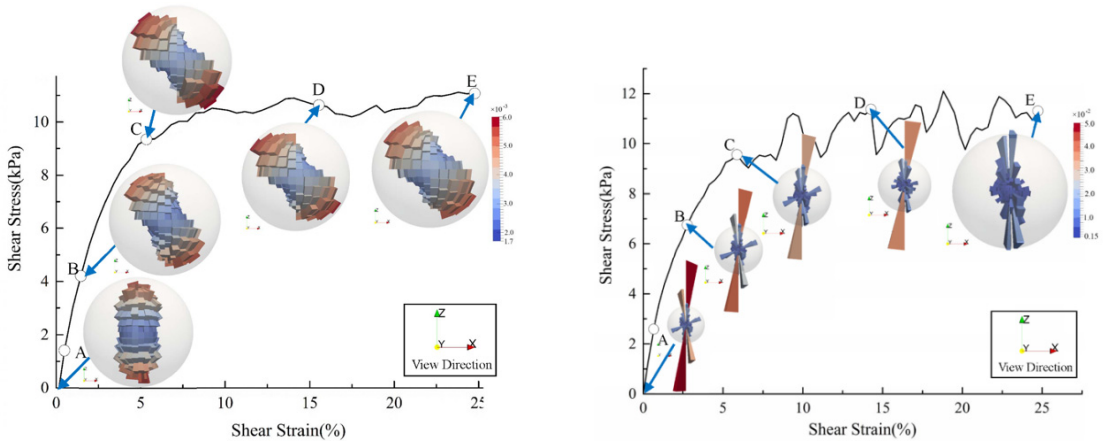

(a) (b)

Fig. 15 Evolution of rose diagram of normal contact force inside the localization band during the shearing process: (a) soil sample, normal stress is 14 kPa and the radius of the scaling sphere is 6×10^{-3}; (b) S-RM sample, normal stress is 11 kPa and the radius of the scaling sphere is 1.5×10^{-2}

forces in the soil sample is much more uniform than that in the S-RM sample.

For the soil sample (Fig. 15(a)), the primary normal contact forces distribute along the vertical direction at the beginning of the shearing process. Once the horizontal shear begins, the direction of the primary normal contact forces rotates against the shear direction, until at the plastic stage the rotation reaches its maximum value, and then remains stable during the following process.

In the S-RM sample, stronger force chains might form between rock blocks, which may have strongly controls the distribution of contact forces, and make the contact force concentrate in some directions (Fig. 15(b)). During the shearing process, the movement, rotation and rearrangement of the rock blocks can destroy the original structure of the stronger force chains, and the concentration of contact force gradually decreases.

7. Conclusions

Based on the previous in-situ direct shear test, the mechanical behavior of soil and especially S-RM are studied via the 3D DEM numerical tests. To simulate the polyhedron rock blocks of S-RM, a non-overlapping combination method of sphere assembly is used in the DEM model of S-RM. To study the strain of the spherical particle system at the meso scale, use of the volumetric strain based on the Voronoi cell of the particle is proposed.

According to the in-situ tests of the soil and S-RM samples, the meso-mechanical parameters of the studied soil and soil-rock interface have been obtained. Then, using these parameters in DEM numerical tests, qualitatively good results have been obtained when compared with results form the in-situ tests.

Deformation localization is common in the shearing process of geotechnical materials. Rotation, occlusion, dilatation and self-organizing force chain were remarkable phenomena of localization band. Using the DEM numerical tests, the mechanical behavior such as rotation, dilatation and self-organizing of force chain of soil and S-RM samples during the shearing process are also analysed. Rotation and overcoming of the occlusion of larger rock blocks in the localization band are more difficult than for small soil particles, which is the most important reason for higher shear strength of the S-RM sample relative to that of soil sample.

Rock blocks in the S-RM caused the contact force chain to be much more non-uniform than that in the soil sample. During the shearing process, stress axes rotated to the opposite direction of the shear, leading to anisotropy of the contact force. This type of anisotropy maximized at the initiation of the plastic deformation, decreasing in the subsequent process.

Acknowledgments

This study was supported by the project of "Natural Science Foundation of China (51479095, 51109117)" and "State Key Laboratory of Hydroscience and Engineering Project (2013-KY-4)", to which we hereby express our sincere gratitude.

References

Chang, Y.-L., Chu, B.-L. and Lin, S.-S. (2003), "Numerical simulation of gravel deposits using mult-circle granular model", *J. Chinese Inst. Eng.*, **26**(5), 681-694.

Cundall, P.A. and Strack, O.D.L. (1979), "A discrete numerical model for granular assemblies", *Géotechnique*, **29**(1), 47-65.

Ergenzinger, C., Seifried, R. and Eberhard, P. (2012), "A discrete element model predicting the strength of ballast stones", *Comput. Struct.*, **108-109**, 3-13.

Evans, T.M. and Frost, J.D. (2010), "Multiscale investigation of shear bands in sand: Physical and numerical experiments", *Int. J. Numer. Anal. Method. Geomech.*, **34**(15), 1634-1650.

Galindo-Torres, S.A. and Pedroso, D.M. (2010), "Molecular dynamics simulations of complex-shaped particles using Voronoi-based spheropolydra", *Phys. Review E*, **81**, 061303.

Garcia, X., Latham, J.-P., Xiang, J. and Harrison, J.P. (2009), "A clustered overlapping sphere algorithm to represent real particles in discrete element modelling", *Géotechnique*, **59**(9), 779-784.

Ishida, T., Kanagawa, T. and Kanaori, Y. (2010), "Source distribution of acoustic emissions during an in-situ direct shear test: Implications for an analog model of seismogenic faulting in an inhomogeneous", *Eng. Geol.*, **110**(3-4), 66-76.

Jerier, J.-F., Richefeu, V., Imbault, D. and Donzé, F.V. (2010), "Packing spherical discrete elements for large scale simulations", *Comput. Method. Appl. Mech. Eng.*, **199**(25-28), 1668-1676.
Kozicki, J. and Donzé, F.V. (2008), "A new open-source software developed for numerical simulations using discrete modeling methods", *Comput. Method. Appl. Mech. Eng.*, **197**(49-50), 4429-4443.
Kozicki, J. and Donzé, F.V. (2009), "YADE-OPEN DEM: An open-source software using discrete element methods to simulate granular material", *Eng. Computat.*, **26**(7), 786-805.
Matsushima, T., Katagiri, J., Uesugi, K., Tsuchiyama, A. and Nakanok, T. (2009), "3D shape characterization and image-based DEM simulation of the lunar soil simulant FJS-1", *J. Aerosp. Eng., ASCE*, **22**(1), 15-23.
Mcdowell, G.R. and Harireche, O. (2002), "Discrete element modelling of yielding and normal compression of sand", *Géotechnique*, **52**(4), 299-304.
Morgenstern, N.R. and Tchalenko, J.S. (1967), "Microscopic structure in kaolin subjected to direct shear", *Géotechnique*, **17**(4), 309-328.
Oyanguren, P.R., Nicieza, C.G., Fernández, M.I.Á. and Palacio, C.G. (2008), "Stability analysis of Llerin rockfill dam: An in situ direct shear test", *Eng. Geol.*, **100**(3-4), 120-130.
Potyondy, D.O. and Cundall, P.A. (2004), "A bonded-particle model for rock", *Int. J. Rock Mech. Min. Sci.*, **41**(8), 1329-1364.
Rycroft, C.H. (2009), "Voro++: A three-dimensional Voronoi cell library in *C*++", *Chaos*, **19**, 041111.
Scholtes, L. and Donzé, F.V. (2012), "Modelling progressive failure in fractured rock masses using a 3D discrete element method", *Int. J. Rock Mech. Min. Sci.*, **52**, 18-30.
Sullivan, C.O. (2008), "Particle-based discrete element modelling: A geomechanics overview", *Proceedings of the 12th International Conference of International Association for Computer Method and Advances in Geomechanics* (*IACMAG*), Goa, India, October, pp. 498-505.
Terzaghi, K. and Peck, R.B. (1848), *Soil Mechanics in Engineering Practice*, Wiley, New York, NY, USA.
Widuliński, L., Kozicki, J. and Tejchman, J. (2009), "Numerical simulation of triaxial test with sand using DEM", *Arch. Hydro-Eng. Environ. Mech.*, **56**(3-4), 149-171.
Xu, W.J. (2008), "Study on meso-structural mechanics(M-SM) of soil-rock mixture (S-RM) and its slope stability", Ph.D. Dissertation; Institute of Geology and Geophysics, Chinese Academy of Sciences, Beijing, China. [In Chinese]
Xu, W.J., Xu, Q. and Hu, R.L. (2011), "Study on the shear strength of soil-rock mixture by large scale direct shear test", *Int. J. Rock Mech. Min. Sci.*, **48**(8), 1235-1247.

CC